

The Effect of the Electron–Electron Interaction in Above-Threshold Double Ionization

M. Lein^{1,2}, E. K. U. Gross³, and V. Engel²

¹ *Blackett Laboratory, Imperial College of Science, Technology, and Medicine, London, SW7 2BW UK*

² *Institut für Physikalische Chemie, Universität Würzburg, Am Hubland, Würzburg, D-97074 Germany*

³ *Institut für Theoretische Physik, Freie Universität Berlin, Arnimallee 14, Berlin, D-14195 Germany*

e-mail: hardy@physik.fu-berlin.de

Received September 12, 2001

Abstract—Electron and ion momentum spectra following double ionization by 250 nm laser pulses are numerically obtained for several two-electron systems: a He model atom; the same system without electron–electron interaction; a H[−] model ion. The two-electron momentum distributions differ qualitatively from system to system. However, the recoil-ion spectra are qualitatively similar. In all cases, they exhibit a peak structure due to above-threshold double ionization.

It is known for many years now from experiment and theory that double ionization of atoms in intense laser pulses is strongly enhanced by electron–electron correlation [1–3]. Recently, the interest into the phenomenon has been renewed as a series of experiments gave new insight into the double-ionization mechanism [4–7]. In these experiments, a crucial element is the measurement of the recoil momenta of the doubly charged ions or, in a more sophisticated setup, the measurement of momenta for electrons which are emitted in coincidence with the doubly charged ions. In a very good approximation, the total momentum of an atom is conserved when exposed to laser irradiation because the photon momentum is negligible. Therefore, the recoil-ion momentum p^{2+} is related to the electron momenta p_1 and p_2 by $p^{2+} = -(p_1 + p_2)$ and thus gives valuable information about the electron momenta.

We have recently predicted [8] that the two-electron analogue of above-threshold ionization (ATI, see [9, 10]) can be observed in the electron spectra and also in the recoil-ion momentum spectra. Above-threshold double ionization (ATDI) manifests itself as a peak structure in the spectra where the different peaks correspond to different numbers of absorbed photons. Our model calculation predicted that the effect is observable for pulses of 400 and 250 nm wavelength. It is important to note that an ATDI peak structure appears not only in the two-electron spectra, but also in the recoil-ion momentum spectra. These can be measured with much less effort than correlated two-particle distributions since no coincidence setup is needed. The full three-dimensional calculation by Parker *et al.* has also predicted the appearance of ATDI structures [11]. Their calculation, however, was carried out for wavelengths around 20 nm [11].

In this paper, we extend our study to investigate in how far the electron–electron interaction affects the ATDI structures. To that end, the calculation is per-

formed not only for a He model atom with interacting electrons, but also for a system with the same nuclear charge but no electron–electron repulsion. Furthermore, we study the behavior of a H[−] model ion. The electrons are more loosely bound in H[−]. Hence, under similar conditions, the ionization probability is much larger and the ionization is dominated by the sequential process in which both electrons are ejected independently of each other. Therefore, the H[−] will take an intermediate position where the electron–electron interaction is present, but not as important as in the He atom.

The dynamics of the two-electron model system, driven by an electric field $E(t)$, is governed by the Hamiltonian

$$H = \frac{p_1^2}{2} + \frac{p_2^2}{2} + (p_1 + p_2)A(t) - \frac{Z}{\sqrt{z_1^2 + 1}} - \frac{Z}{\sqrt{z_2^2 + 1}} + \frac{\lambda}{\sqrt{(z_1 - z_2)^2 + 1}}, \quad (1)$$

with $A(t) = -\int_0^t E(t')dt'$. Here, the nuclear charge is $Z = 2$ for He, and $Z = 1$ for H[−]. The parameter λ measures the electron–electron interaction and is set to 1 except in the case of the non-interacting He atom where $\lambda = 0$. We integrate the time-dependent Schrödinger equation for the two-electron wave function $\Psi(z_1, z_2, t)$ by employing the split-operator method [12]. The wave function is numerically represented on a two-dimensional grid.

The calculation of the final two-electron momentum distribution is rather demanding. This is because the wave function reaches a spatial extension of several hundred atomic units within a few optical cycles. For realistic laser pulses, the grid cannot be made large enough to contain the whole wave function, and one

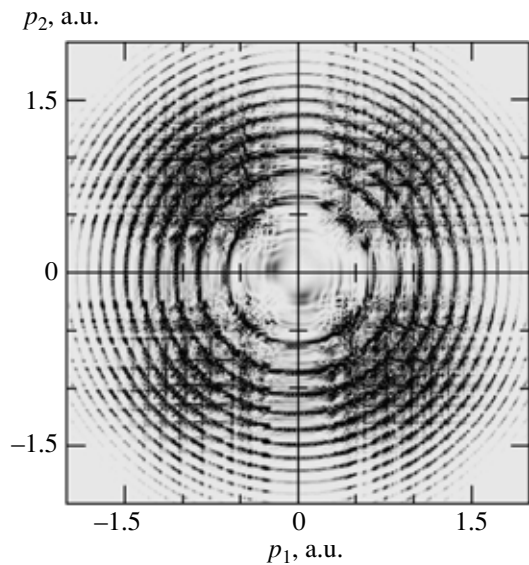


Fig. 1. Two-electron momentum distribution for double ionization of the He model atom by a 250 nm pulse with intensity 10^{15} W/cm 2 .

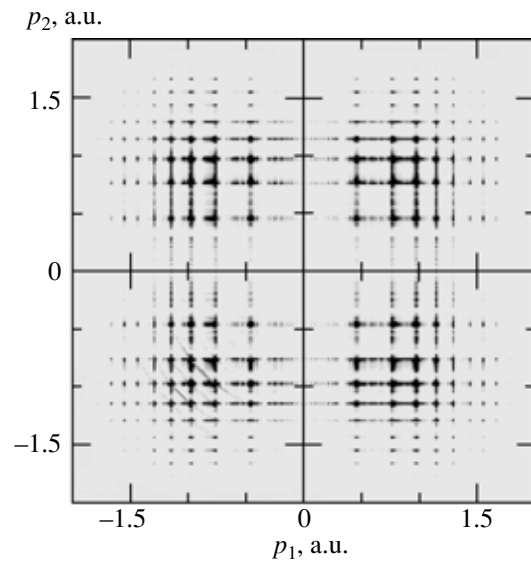


Fig. 2. Two-electron momentum distribution for double ionization of the He model atom with non-interacting electrons by a 250 nm pulse with intensity 10^{15} W/cm 2 .

uses absorbing boundaries to absorb the outgoing electron flux. The calculation of final electron spectra requires to store the information about the momenta of the outgoing electrons. We use the method developed in our previous work [13], i.e., we divide the configuration space into three regions, one corresponding to the neutral atom (or intact H $^-$ ion, respectively), one corresponding to the singly ionized system, and one corresponding to the doubly ionized system. In the double-ionization part, both electrons are far away from the nucleus, and typically far from each other as well. Hence, in this region, the particle–particle interactions can be neglected and the wave-function propagation can be accomplished by multiplications in momentum space. Similarly, in the single-ionization region, the same is true for one of the two electrons. In this work, the boundary of the inner part is located at ± 200 a.u. Note that most other publications of numerical two-electron calculations do not show final double-ionization distributions but rather snapshots of the inner region, taken during the action of the laser pulse.

Our calculations are performed for pulses of 250 nm wavelength and a duration of 24 optical cycles. For He and its non-interacting variant, we use an intensity of 10^{15} W/cm 2 . For H $^-$, we use a reduced intensity of 3×10^{14} W/cm 2 in order not to ionize this weakly bound system in a too short time. The pulse shape is chosen such that the electric-field envelope is trapezoidal with 6-cycle leading and falling ramps. By using this pulse shape we avoid unrealistic pulse shape effects on the final momentum spectra as we will briefly show in the following. Assume that an ion of charge q is created with zero initial velocity at time t_0 during the action of

a trapezoidal pulse

$$E(t) = \begin{cases} E_0 \frac{t}{t_1} \sin(\omega t), & 0 \leq t \leq t_1 \\ E_0 \sin(\omega t), & t_1 < t \leq t_2 \\ E_0 \left(1 - \frac{t-t_2}{t_3-t_2}\right) \sin(\omega t), & t_2 < t \leq t_3 \\ 0, & t > t_3. \end{cases} \quad (2)$$

After ionization, assume that the ion is accelerated according to the classical equation of motion for a free particle exposed to the laser field. Then, for $t_1 < t_0 < t_2$, it is straightforward to show that the final ion momentum is

$$p_{\text{ion}} = \frac{qE_0}{\omega} \cos(\omega t_0) + \frac{qE_0}{\omega^2(t_3-t_2)} [\sin(\omega t_2) - \sin(\omega t_3)]. \quad (3)$$

In our case, t_2 and t_3 are such that the second term vanishes. The remaining first term equals the ion drift velocity around mid-pulse where the field amplitude is constant and the ion velocity oscillates with frequency ω around a mean value. The equality of final momentum and drift momentum does not hold in general, but it does hold in the adiabatic limit of long pulses. This case usually applies to the pulses used in experiment. Quantum mechanical computer simulations, on the other hand, are often restricted to much shorter pulse dura-

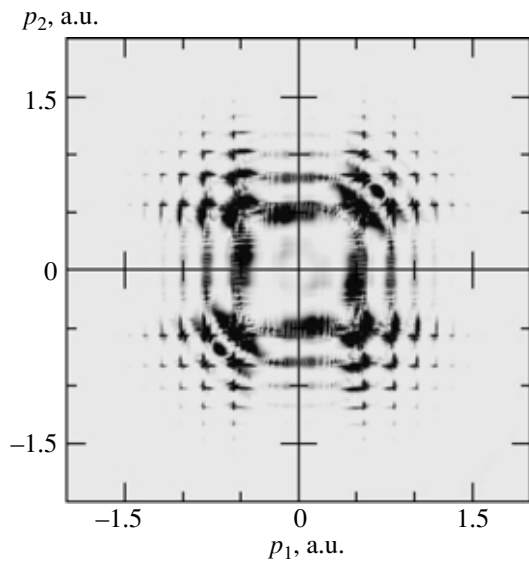


Fig. 3. Two-electron momentum distribution for double ionization of the H^- model ion by a 250 nm pulse with intensity $3 \times 10^{14} \text{ W/cm}^2$.

tions. The trapezoidal envelope shape, however, avoids artificial short-pulse effects on the final momenta.

Figures 1–3 show the final momentum distributions for double ionization. They are taken after a total prop-

agation time of 36 optical cycles (employing a 24-cycle pulse plus 12 cycles field-free propagation). Figure 1 gives the result for the He model atom. We find the typical ATDI ring structure as we have explained in detail in our previous publication [8]. Each ring is a line of

constant total energy $E_{\text{kin}} = p_1^2/2 + p_2^2/2$. The different rings correspond to a different number of absorbed photons. When the interaction between the two electrons is switched off, we obtain the distribution of Fig. 2. Here, there is no ring structure. Instead, we find a cross-like pattern. The maxima of this distribution are located at the crossing points of horizontal and vertical lines. Clearly, the spectrum is the product of two identical one-electron spectra exhibiting the typical one-electron ATI peaks. This type of double ionization is sequential. Contrary to this non-interacting two-electron system, in the interacting system, energy can be dynamically transferred from one electron to the other. Then, density appears essentially everywhere along the lines of constant total energy. Both the ring structure and the cross-like pattern were found in the short-wavelength calculation of [11] as well. Figure 3 displays the distribution for the H^- ion. This distribution takes an intermediate position: It consists of maxima which are arranged according to the cross pattern, but these maxima tend to become connected along circles. Due to the quicker ionization of H^- , the maxima are broadened out

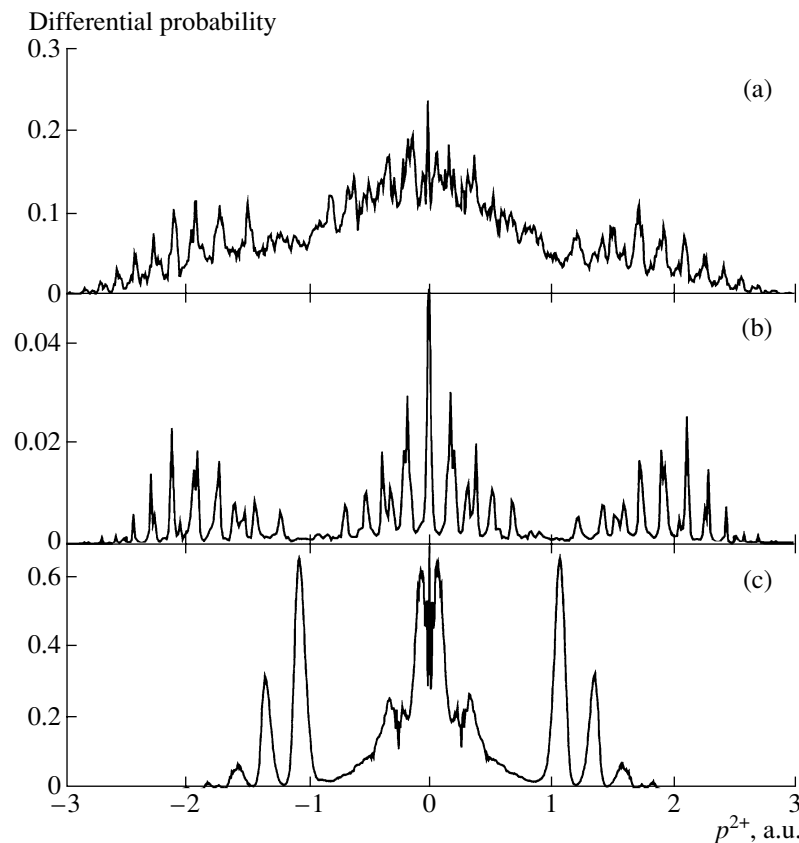


Fig. 4. Recoil-ion momentum distributions for double ionization. Panels (a), (b), and (c) correspond to Figs. 1, 2, and 3, respectively.

as compared to He, although the laser intensity is chosen lower for H^- .

In panels (a–c) of Fig. 4, we present the recoil-ion spectra. They show the momentum distribution of the ejected He^{2+} ions or H^+ ions, respectively. There is a well-defined peak structure in all cases. In the region of large absolute recoil momenta, i.e., $|p^{2+}| \geq 1$ a.u., one can easily check that the peaks are separated by the photon energy $\hbar\omega$ if for each peak, a corresponding energy value of $E_{\text{kin}} = (p^{2+})^2/4$ is calculated. We have explained the appearance of these peaks in [8]. The explanation, however, was based on the ring structure in the two-electron distribution. Surprisingly, the system with non-interacting electrons shows the same peak structure in the recoil-ion spectrum [see Fig. 4b] although it has a two-electron momentum distribution with no ring structure. Apparently, the reason is the following: The regions giving rise to the peaks at large absolute p^{2+} are those where p_1 and p_2 are both large and positive or both large and negative. As Fig. 2 shows, there is large probability in these regions. Although the maxima are clearly separated from each other, they can be thought of as lying on concentric circles. The maxima that lie on the same circle are close enough to each other to produce a single peak in the recoil-ion spectrum instead of several ones.

We conclude that the electron–electron interaction changes the two-electron momentum spectrum qualitatively as it causes the appearance ATDI rings. These rings are not found for non-interacting electrons. In double ionization of H^- , a ring structure is observed, but it is less pronounced than for He. For all systems, how-

ever, the recoil-ion momentum spectra exhibit the same peak structure in the sense that the separation of the peaks is related to the photon energy by the same formula. This ATDI structure seems to be quite robust. Therefore, we expect that it will be observed in experiment in the near future.

This work was supported by the Deutsche Forschungsgemeinschaft and the Fonds der Chemischen Industrie.

REFERENCES

1. Fittinghoff, D.N., Bolton, P.R., Chang, B., and Kulander, K.C., 1992, *Phys. Rev. Lett.*, **69**, 2642.
2. Walker, B. *et al.*, 1994, *Phys. Rev. Lett.*, **73**, 1227.
3. Becker, A. and Faisal, F.H.M., 1996, *J. Phys. B*, **29**, L197.
4. Moshhammer, R. *et al.*, 2000, *Phys. Rev. Lett.*, **84**, 447.
5. Weber, Th. *et al.*, 2000, *Phys. Rev. Lett.*, **84**, 443.
6. Weber, Th. *et al.*, 2000, *Nature*, **405**, 658.
7. Witzel, B., Papadogiannis, N.A., and Charalambidis, D., 2000, *Phys. Rev. Lett.*, **85**, 2268.
8. Lein, M., Gross, E.K.U., and Engel, V., 2001, *Phys. Rev. A*, **64**, 023406.
9. Agostini, P. *et al.*, 1979, *Phys. Rev. Lett.*, **42**, 1127.
10. Eberly, J.H., Javanainen, J., and Rzazewski, K., 1991, *Phys. Rep.*, **204**, 331.
11. Parker, S. *et al.*, 2001, *J. Phys. B*, **34**, L69.
12. Feit, M.D., Fleck, J.A., and Steiger, A., 1982, *J. Comput. Phys.*, **47**, 412.
13. Lein, M., Gross, E.K.U., and Engel, V., 2000, *Phys. Rev. Lett.*, **85**, 4707.